International Journal of Innovation in Science and Mathematics
Volume 8, Issue 2, ISSN (Online): 2347–9051

Modification of Polybutadiene Obtained from Scrap Tire as a Cheap Corrosion Inhibitor

Khawlah S. Burghal *, Hassan T. Abdulsahib and Sameerah A. Zearah
Chemistry Department, Science College, Basrah University, Basrah, Iraq.
*Corresponding author email id: lolaby2005@yahoo.com

Date of publication (dd/mm/yyyy): 11/04/2020

Abstract **– The major use of Polybutadiene is in treads and sidewalls of tyres wasted tires do not decompose, become a heavy burden. Thewasted modified byhalogenated ground tire rubber, at that point modified with diamine item was characterized by FTIR, X-ray Diffractometry and FESEM. And the thermal properties (TGA,DSC) indicated the prepared compound was thermally steady until 202˚C. The electrochemical strategy used Tafel plot to measure the effectiveness of inhibitor. The productivity of the readied consumption inhibitor for carbon steel was estimated by utilizing corrosive media (1N HCl) as environment condition and the inhibitor focus seemed to be (0, 10, 20 and 30 ppm). Components impact on the step of erosion like temperature (298, 308, and 328 K) and concentration (10, 20 and 30 ppm) of inhibitor were examined. From the developed outcomes numerous elements were determined that decided the ability of the inhibitor like consumption rate, charge move opposition and inhibitor productivity It was seen that the corrosion rate and charge move of the carbon steel for the inhibitor increment with increment of temperature and reduction with increment of the inhibitor fixation in a similar temperature. The outcomes demonstrated that the inhibitor had high hindrance in diminishing the consumption rate. The restraint effectiveness (% IE) arrived at 91.13% for the 30 ppm focus at 323 K.**

Keywords **– Polybutadiene, Scrap Tire, Corrosion, Inhibitor.**

I. INTRODUCTION

The strong waste administration is positively a significant test everywhere throughout the world [1]. The expanding number of vehicles in recent decades has prompted a tremendous creation of waste tires all through the world. "Constantly 2030, around 1200 million tires are expected upon to be wasted every year. Evaluated information demonstrate that in excess of 17 million tons of tires are pulled back from utilize each year everywhere throughout the world, of which 3.3 million comes from the European Union [2]. Since squandered tires don't decay, become a substantial weight, the purported "Dark Pollution", their immense amassing causes genuine natural issues [3], some of which incorporate possessing huge regions for support, making unseemly visual scenes Recycling waste tires can extraordinarily diminish the ecological issues brought about by their collection. Therefore, reusing of waste rubbers searching for new methods of used tires recycling is a widespread topic of research conducted by industries and scientific centers all over the world [4, 5]. The material recycling, quiet conducted only on a small scale, is a very good alternative for energy recovery [6]. Burning of waste tires, mainly in cement and power plants enables the recovery of only about 37 % of energy used for the manufacture of new tires. Nowadays, industries and research centers in the EU and the whole world are searching for new, alternative and economically right industrial scale methods of waste rubber recycling. Destroyed rubber compounds have been used as filers or substitutes of elastomers in elastic mixes, thermoplastic elastomers, thermoplastic organizations, epoxy saps, and so on [7, 8]. "Corrosion inhibition is one of the "issues "that has been widely considered and examined on the grounds that it is one of the most valuable approaches to, protect, materials with minimal cost and high proficiency [9]. "Corrosion of metals is a serious environmental issue that has been given sufficient consideration in the oil and gas industries in light of the fact

that, during modern procedures, for example, corrosive cleaning and carving, metal surfaces are regularly reached acidic medium, demonstrating that the utilization of inhibitors is essential [10]. The fruitful utilization of normally happening substances to repress the erosion of metals in acidic and antacid conditions has been accounted for by some exploration bunches, "inhibiting the anodic reaction of the steel bar surface". The mechanism of the corrosion inhibition in reinforced concrete is that the electrochemical reaction. The general corrosion rate might be estimated using immersion tests or electrochemical tests. Electrochemical tests are quick and can be utilized for a fast screening of natural impacts, for example, temperature and electrolyte arrangement. The utilization of inhibitors is one of the most reasonable strategies for security against corrosion. The concentration of a given inhibitor needed to protect a metal will depends on number of factors: such as (i) composition of the environment, (ii) temperature, (iii) velocity of the liquid, (iv) the presence or absence in the metal of internal or external stresses, (v) composition of the metal Corrosion inhibitors are frequently used to slow down the Corrosion [11]. It is important to incorporate corrosion inhibitors in the protective coatings as their expansion in the electrolyte isn't constantly conceivable. Most commonly used consumption inhibitors of the most recent decades are the chromates, which have high proficiency in watery media and are utilized for a wide scope of metals and alloys [12]. The use of inhibitor as a as a cost-effective and most straight forward strategy for stifling metal erosion is a typical certainty. Natural mixes top the outline of metal consumption inhibitors at present, Nevertheless, a portion of these natural mixes are viewed as hostile to the biological system and costly, Polymers have been recognized as potential ecofriendly and reasonable erosion inhibitors [13, 14]. Organic inhibitor is applied broadly to protection metals from consumption in numerous forceful acidic media. In the present investigation squander ground tire elastic were halogenated by bromine in CCl4 utilizing paraphynlene diamine (PPD) to create (polybutadiene-g-paraphynlene diamine), the produce compound was tried as consumption inhibitor.

II. MATERIALS AND METHODS

2.1. *Materials*

C-steel (C1010) was acquired from Metal Samples (USA) was utilized with the accompanying structure by rate weight: C = 0.13, Mn = 0.3, Si = 0.37, P = 0.04, S = 0.05, Cr = 0.1, Ni = 0.3, Cu = 0.3, AS = 0.08 and the rest of Fe. Scrap tires were gathered from Basra scrap tire dump site, Iraq, HCl were gotten from Aldrich Chemical and p-phynlene diamine from Aldrich.

2.2. *Experimental Methods*

2.2.1. *Electrochemical Measurements*

The electrochemical estimations were performed utilizing a potentiostat/ galvanostat (ACM) associated with a PC. A three "electrode" cell gathering, consist of a C-steel bar inserted in araldite as the working cathode (WE), "a platinum sheet as the counter terminal (CE)" and an saturated calomel electrode as the reference electrode (RE), was utilized for the "electrochemical estimations". The temperature of the electrolyte was kept up at the necessary temperature utilizing a water" bath. Before immersion in the test solutions, the WE was cleaned with a cleaning machine utilizing emery paper from 600 to 1200 evaluation until an identical representation was gotten. At that point, the WE was washed with refined water at that point immersed in acetone for 1 moment in a ultrasonic more clean. The WE terminal was arranged legitimately before electrochemical estimations at that

point submerged in the test arrangement at open circuit potential for one hour until a consistent state potential was gotten before impedance and polarization estimations were performed. All estimates were acted in circulated air through arrangements. From the polarization information, were determined like the level of surface inclusion (θ), the rate restraint effectiveness (% IE), consumption rate and charge move resistance [15].

2.2.2. *Recycling Process*

The tires were washed with water to expel soil and were therefore air dried. The cleaned sides of the tire released from steel breeds were cut into segments with the guide of a hacksaw and later into little pieces utilizing extremely sharp blades. The size of the tire chips were additionally decreased utilizing an electric pounding machine ground tire elastic after treatment (4 g) was added to 25 ml of Bromine in carbon tetra chloride of. The blend was mixed for 2 hours at 25C. The got the halogenated ground tire elastic. It was washed by ethanol and dried at 100 C° for 12 hours [16-18]. (10gm) of p-phynlene diamine was added to 5.0 g of the halogenated ground tire rubber. At that point it was warmed under reflux in oil bathe at 120 C° for 10 and 30 minutes. In the wake of chilling off to room temperature, the acquired item was washed with refined water and dried at 100 C° for 12 hours [19], the proposed component was appeared in (Figure 1), The substance structure of (polybutadiene-g-paraphynlene diamine) was affirmed from their (Figure 2, 3) FT-IR & XRD.

2.2.3. *Characterization for Inhibitor*

Figure 2 shows the FT-IR spectra of (pBut-g-PPD) from the FTIR spectra an It appears at 3379 cm-1 the assimilation of (N-H), 3009 cm^{-1} to (C-H), C=C fragrant shows up in 1512 cm^{-1}. These groups represented the active sites to the dynamic locales where the procedure of adsorption happens because of its charge, which permit framing synthetic or physical bonds. Diffraction is a physical wonder that comprises in electromagnetic waves maintaining a strategic distance from hindrances if the size of the impediments looks at to the wavelength. This phenomenon can be applied to the analysis of materials as the atom plans are placed at comparable distances to X this wonder can be applied to the investigation of materials as the molecule plans are set at practically identical separations to X beam lengths. X beams are electromagnetic waves like light, however whose wavelength is a lot shorter (= 0, 2 - 200 Å) [20]. The X-beam diffraction examples of the (pBut-g-PPD) demonstrated 2θ = 28.09, 31.36, 37.21, 32.49, 31.36, 34.81 and 43.56 that the groups at 2θ = 43° and 34° diminished altogether in the wake of cross linking, and this was trailed by an influenced increment in the crystallinity rate which was seen as 60%.

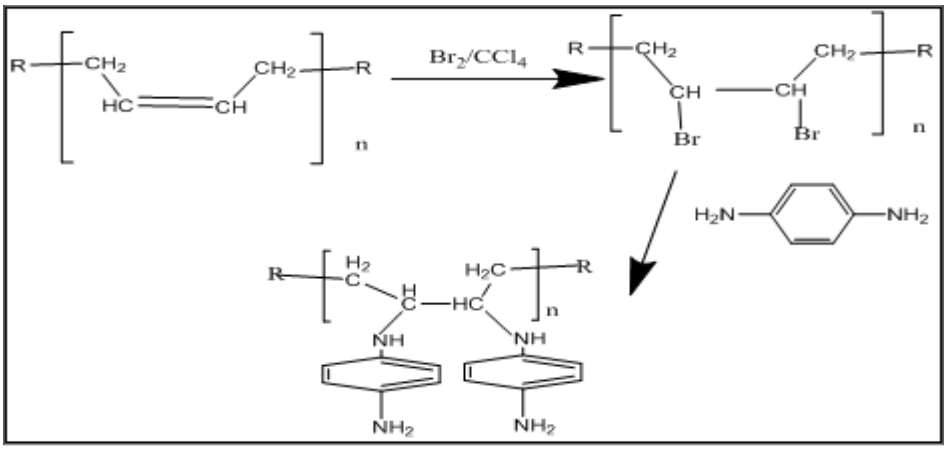

Fig. 1. Polybutadiene-g-paraphynlene diamine.

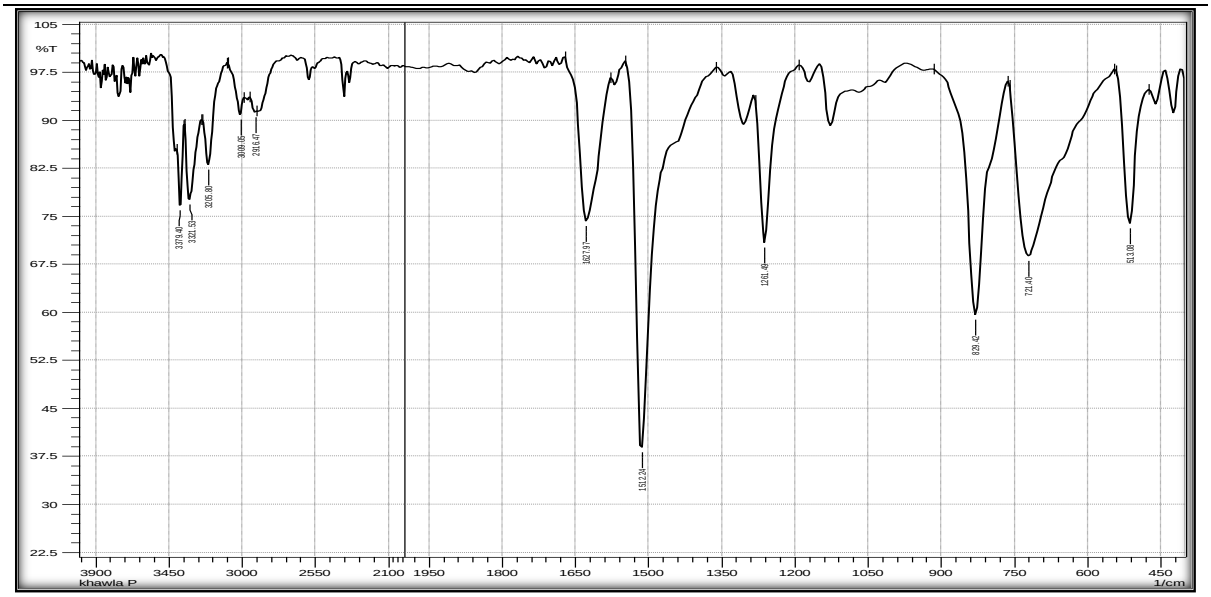

Fig. 2. FT-IR spectrum of polybutadiene-g-paraphynlene diamine.

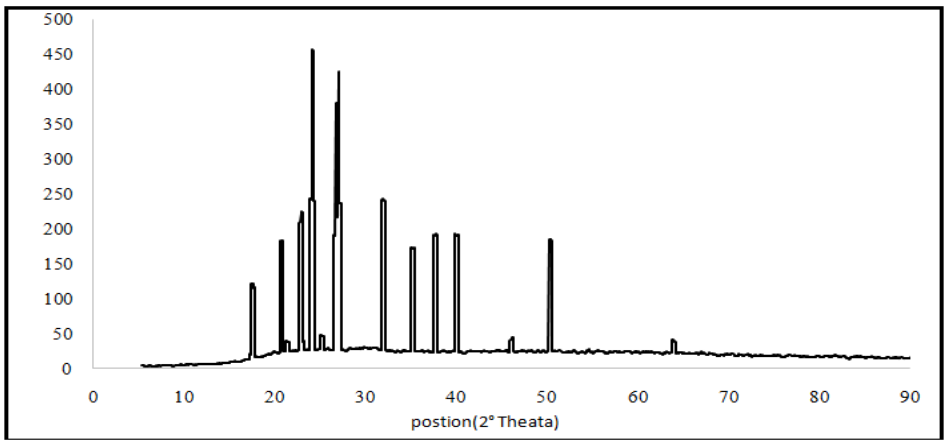

Fig. 3. XRD of polybutadiene-g-paraphynlene diamine.

2.2.4. *Field Emission Scanning Electron Microscopy (FESEM)*

Field Emission Scanning Electron Microscopy (FESEM) was utilized to decide the surface qualities, the surface microstructure and unpleasantness properties. Also, it has been discovered that [21]. (PPD-g-pBut) were stacked haphazardly, and scarcely any layers unmistakable compressions (flower formed).

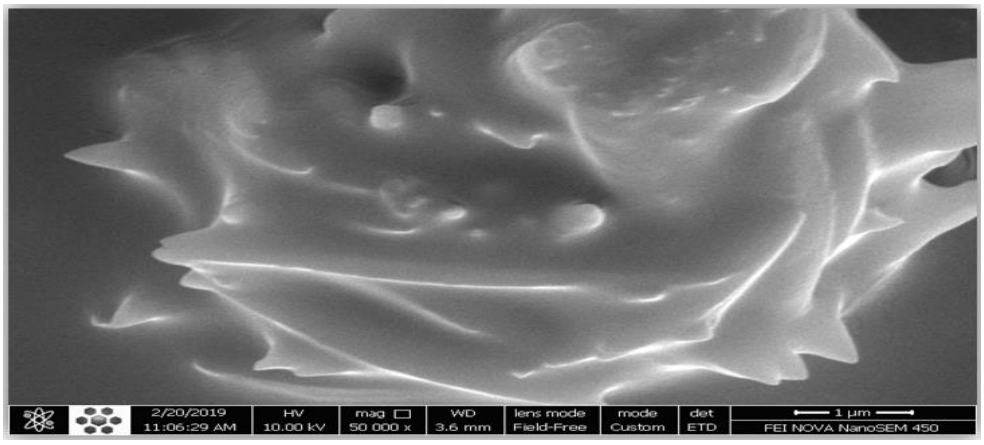

Fig. 5. FESEM of polybutadiene-g-paraphynlene diamine.

III. Results and Discussion

3.1. *Electrochemical Measurements*

3.1.1. *Polarization Measurements (Tafel Method)*

Run of the mill potentiodynamic polarization bends for the C-steel in 1 N HCl in the presence and nonattendance of various convergences of pBut-g-PPD are appeared in (Fig. 5-14). The particular Tafel parameters, inhibition effectiveness (% IE), surface inclusion (θ), Icorr erosion current, consumption rate and charge move obstruction are given in Tables 1. It is clear that the shapes of the Tafel plots for the inhibited electrodes are different from those of uninhibited electrodes. The presence of the inhibitor decreases the current density but does not change other aspects of the behavior Table 1. Tafel parameters for C-steel 1 N HCl in the absence and nearness of various concentrations at various Temp.

Table 1. Tafel plots for C-steel at 323k in 1N HCl (blank) at30 ppm Inhibitor.

Comp.	Con. (ppm)	Temp (k)	CR (mpy)	RΩ	I_{corr} ($\mu A.Cm^{-2}$)	βC A/V	βA A/V	Θ	E%
Blank	1N	298	151.92		23.6	-8.233	16.47		
pBut-g-PPD	10		49.28	30.22	8.50	-7.388	10.7	0.6756	67.56
	20		43.4	31.42	8.18	-7.921	11.01	0.7143	71.43
	30		32.008	34.55	7.44	-6.93	10.72	0.7893	78.93
Blank	1N	308	225.8		27.9	-8.233	9.312		
pBut-g-PPD	10		66.6	22.36	11.5	-7.95	8.394	0.7050	70.50
	20		50.08	23.09	11.1	-8.445	9.684	0.7782	77.82
	30		40.08	29.73	8.64	-7.841	8.686	0.8224	82.24
Blank	1N	323	462.4		79.8				
pBut-g-PPD	10		49.04	30.036	8.46	-9.045	10.59	0.8939	89.39
	20		40.36	35.17	7.31	-8.669	9.628	0.9083	90.83
	30		41	36.31	7.08	-8.586	9.947	0.9113	91.13

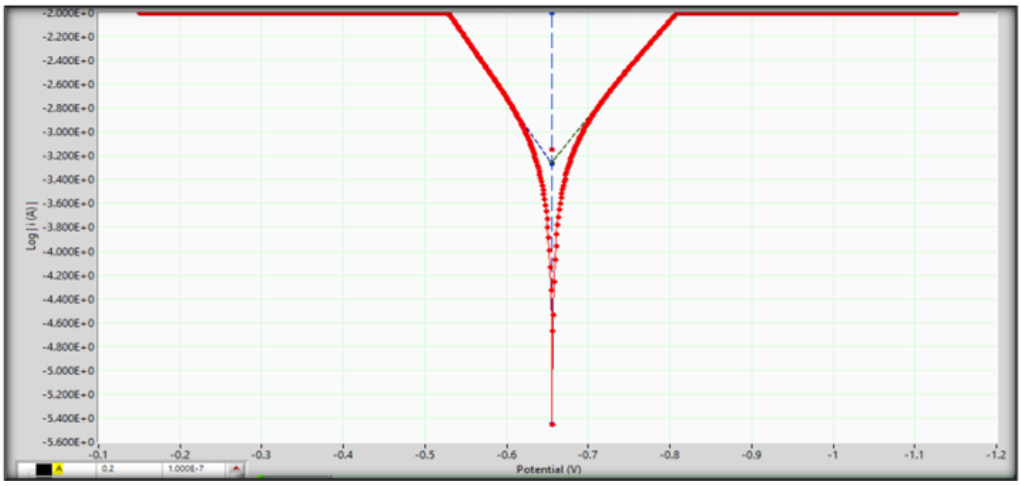

Fig. 5. Tafel Plot of carbon alloy (C1010) in presence and absence of P2 30 ppm inhibitor at 323k.

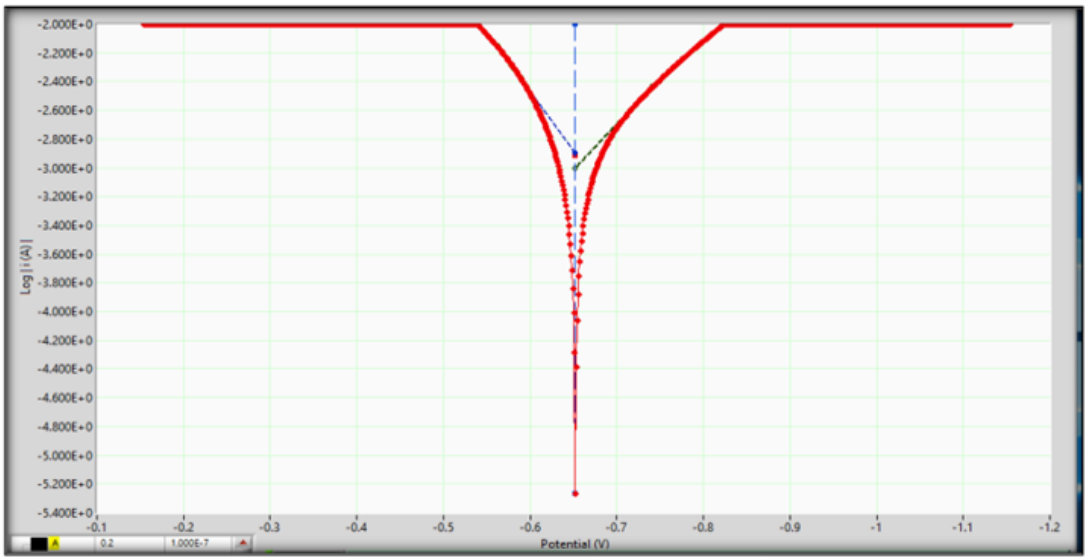

Fig. 6. Tafel plot of carbon steel alloy (C1010) in presence and absence of pBut-g- PPD 10 ppm inhibitor at 298k.

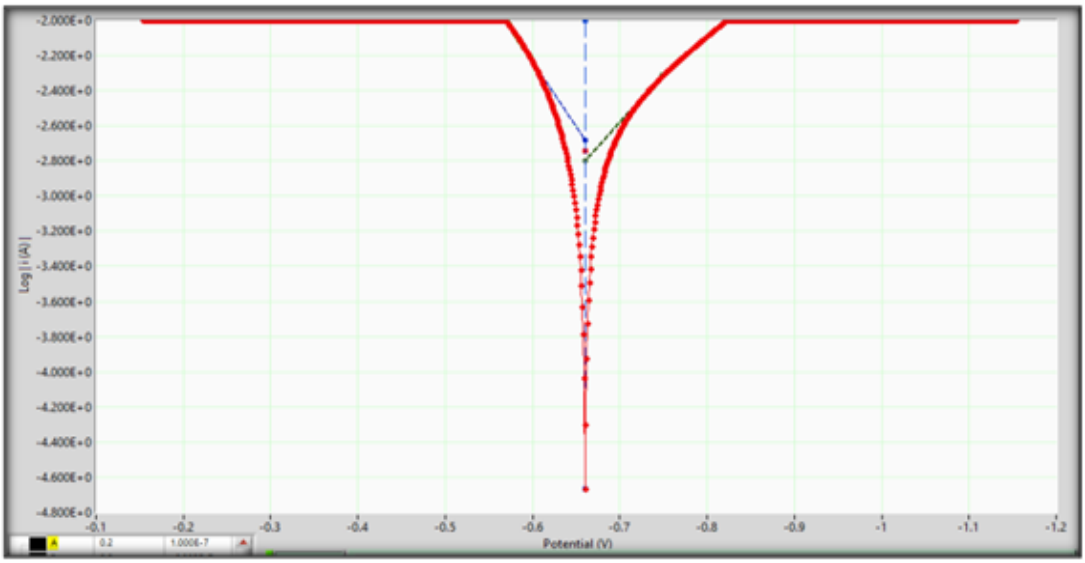

Fig. 7. Tafel plot of carbon steel alloy (C1010) in presence and absence of pBut-g- PPD 20 ppm inhibitor at 298k.

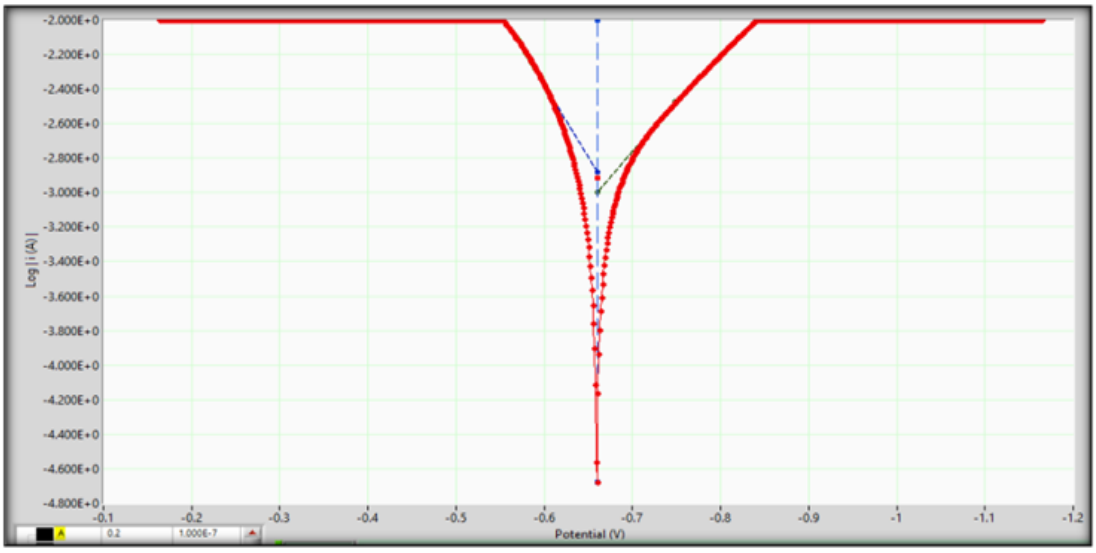

Fig. 8. Tafel plot of carbon steel alloy (C1010) in presence and absence of pBut-g- PPD 30 ppm inhibitor at 298k.

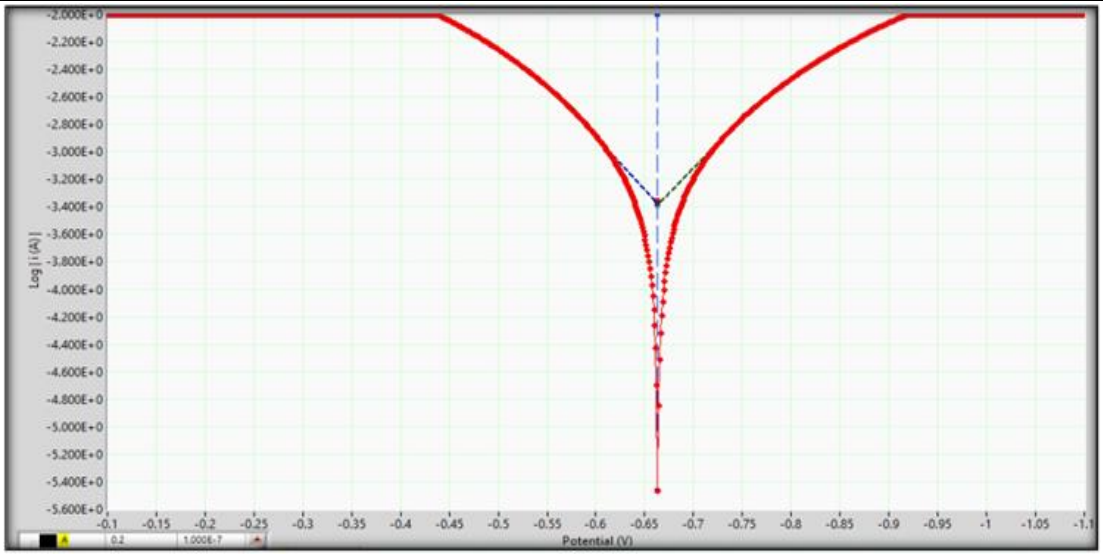

Fig. 9. Tafel plot of carbon steel alloy (C1010) in presence and absence of pBut-g- PPD 10 ppm inhibitor at 318k.

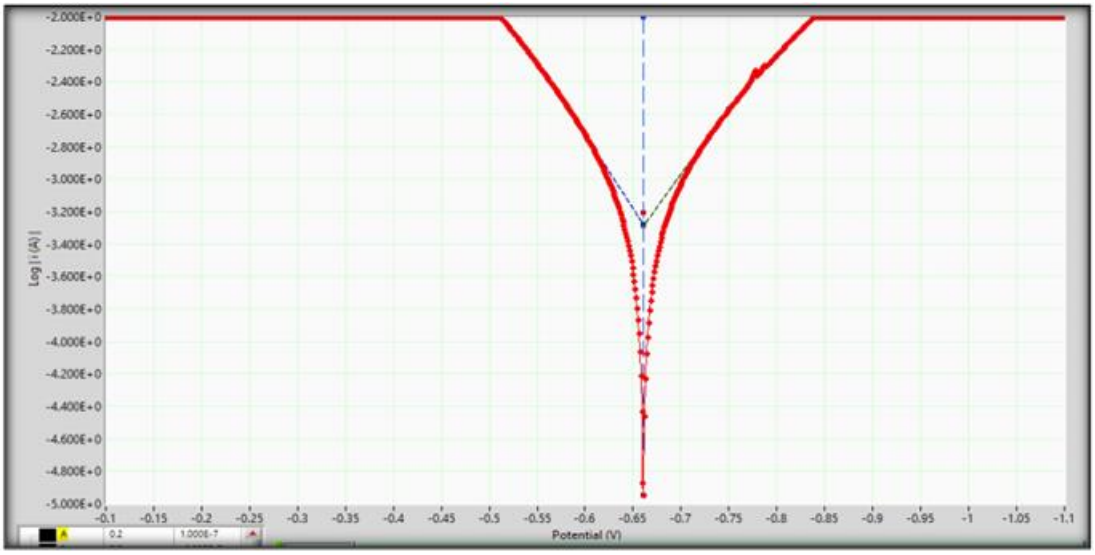

Fig. 10. Tafel plot of carbon steel alloy (C1010) in presence and absence of pBut-g-PPD 20 ppm inhibitor at 318k.

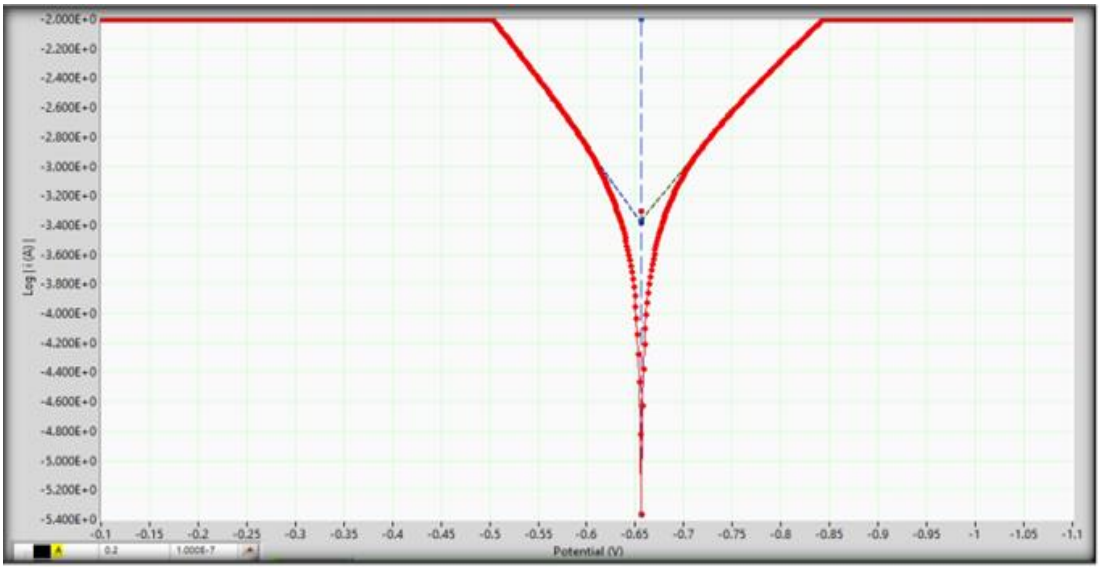

Fig. 11. Tafel plot of carbon steel alloy (C1010) in presence and absence of pBut-g-PPD 30 ppm inhibitor at 318k.

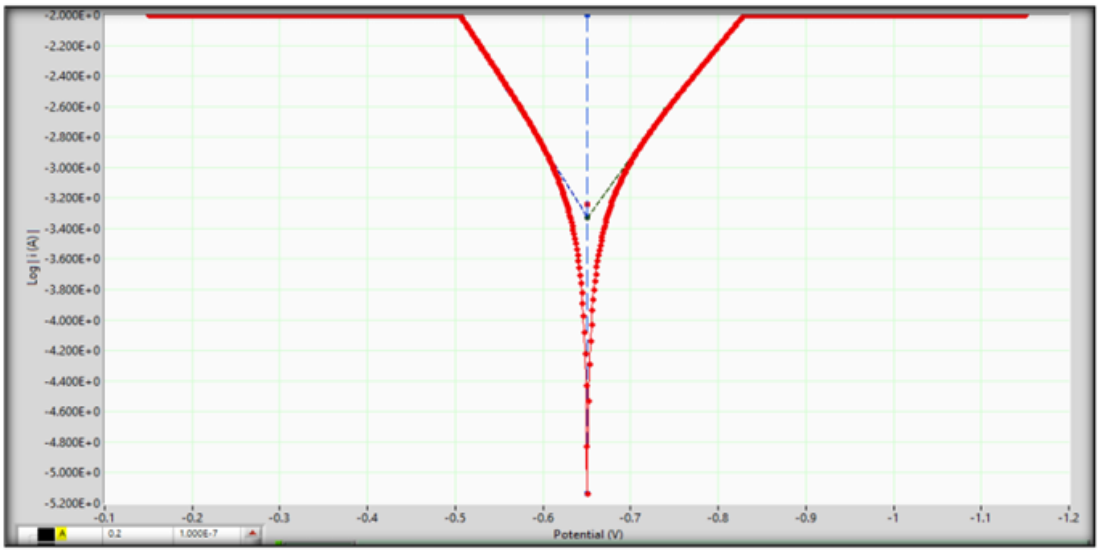

Fig. 12. Tafel plot of carbon steel alloy (C1010) in presence and absence of pBut-g-PPD 10 ppm inhibitor at 323k.

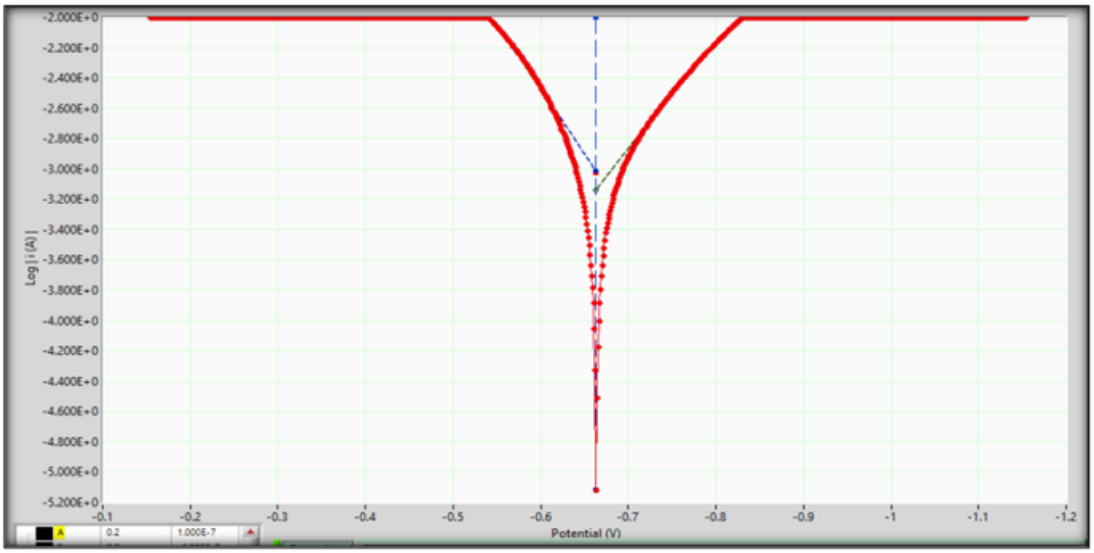

Fig. 13. Tafel plot of carbon steel alloy (C1010) in presence and absence of pBut-g-PPD 20 ppm inhibitor at 323k.

It is obvious from Table 1 that the adsorption of the inhibitor moved the corrosion potential (E_{corr}) in the negative direction, generally a higher E_{corr} and a lower i_{corr} indicate better corrosion protection. The expansion of pBut-g-PPD diminishes both of the Tafel inclines ($ß_a$ and $ß_c$), the anodic and cathodic Tafel takes. This shows pBut-g-PPD is a blended kind inhibitor influencing the iron dissolution and hydrogen advancement.

The decrease of the positive and negative flows within the sight of pBut-g-PPD can be clarified by the obstructing of dynamic destinations by the development of a defensive film on the outside of the terminal. The estimations of the surface inclusion and inhibition proficiency arrived at its greatest at grouping of 30 ppm at 298 k E% 78.93. As can be seen from Table 1, while at 30ppm at 323 E% 91.13 pBut-g-PPD inhibitor enormously diminishes corrosion current with a slight move in the corrosion potential, concerning the corrosion capability of the clear arrangement, the inhibitor can be assigned as a cathodic or anodic type. In the present analysis, and through the distinction consumption potential estimations of corrosion inhibitor in the nearness of the inhibitor, which showed that the contemplated inhibitor is a blended kind inhibitor which is in concurrence with some other studies [22, 23].

3.1.2. *Impact of Temperature*

Temperature is a significant parameter when considering metal degeneration. It is realized that the impact of temperature on the corrosive metal response is profoundly perplexing. The investigation of impact of temperature on the consumption rate to the natural inhibitors on carbon steel alloy were inundated in 1 N hydrochloric corrosive with various fixation (10-30 ppm) of inhibitor at temperature going from 298 K, 308 K, and 328 K, the initiation vitality esteem was determined from Arrhenius equation [23].

$$\text{Ln CR} = \text{Ln A} - \text{Ea/RT} \quad (1)$$

Where : CR = corrosion rate (mpy), E_a = "Activation energy (KJ/ mol),

A = Frequency factor, R= molar gas consistent (8.3143 J.K-1.mol-1),

T = temperature (k).

Figure 13, Figure 14, show great connection between (ln CR) versus (1/T K^{-1}) for without and with inhibitors natural compound in 1NHCl arrangement, straight lines were acquired with slope of (– Ea/R), the activation energy was determined from slope of Arrhenius plot. The Activation energy as the grouping of inhibitor raise which shows physical adsorption [25]. Following equation

$$\text{Ln}\frac{CR}{T} = \text{Ln}\frac{RT}{Nh} + \left(\frac{\Delta S^*}{R}\right) - \left(\frac{\Delta H^*}{RT}\right) \quad (2)$$

Where: CR = Corrosion rate (mpy), ΔH = Enthalpy (KJ/mol), ΔS = Entropy (J/mol, K), R = Molar gas constant (8.3143 $J{\cdot}K^{-1}{\cdot}mol^{-1}$), T = Temperature (K), N = Avogadro number (6.022 × 1023 mol^{-1}); h = Plank, constant (6.62 × 10^{-34} J·s).

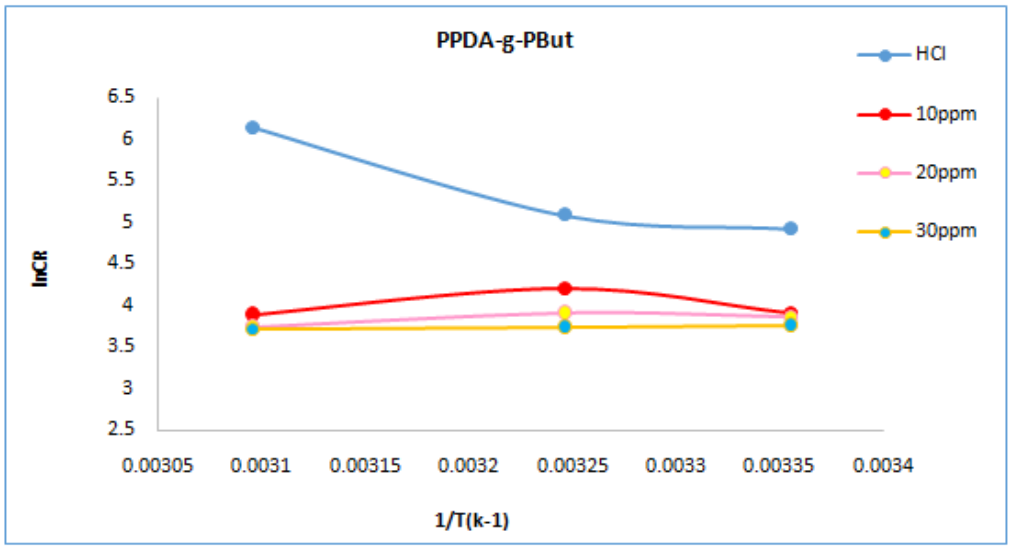

Fig. 15. Calculation of the activation energy for the corrosion reaction of carbon steel alloy (C1010) in presence and the absence of PPDA-g-PBut the inhibitor.

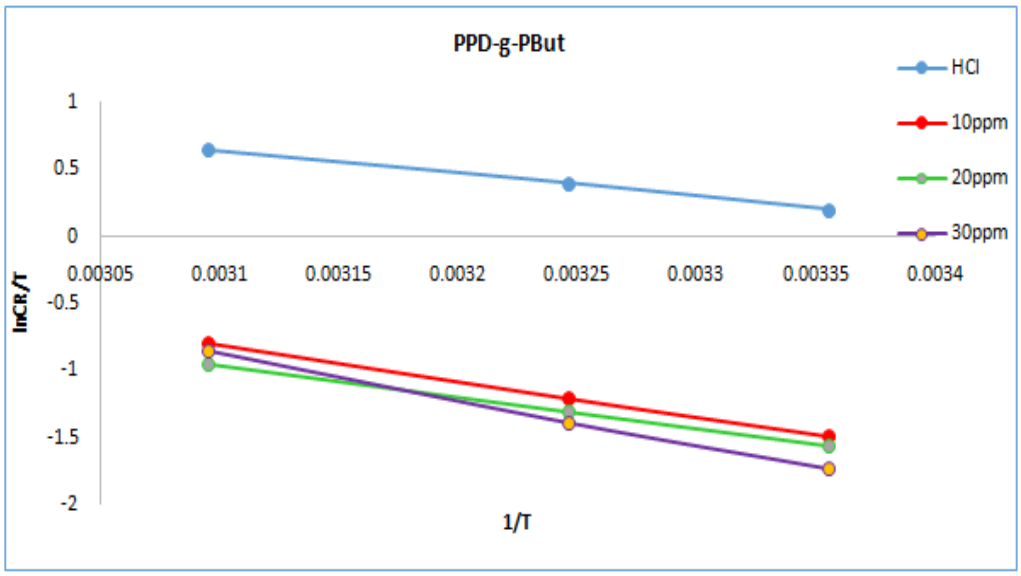

Fig. 16. Calculation of the ΔH^* and ΔS^* for the corrosion reaction of the carbon steel alloy (C1010) in the presence and absence of PPDA-g-PBut the inhibitor.

For carbon steel in with and without inhibitors organic compound in 1N HCl arrangement. Bends demonstrated straight lines with slope ($\Delta H*/R$) and intercept ($\Delta S*/R$).The positive estimation of $\Delta H*$ mirror that the procedure of desorption of the inhibitors superficially is an endothermic procedure (chemical adsorption) and it has been plainly seen that the estimation of $\Delta H*$ expanding as the fixation inhibitor increment. The entropy of initiation in referenced table clear that these qualities expanded emphatically within the sight of inhibitor than in its absence. The expansion of reveals that an increase in disordering takes place from reactant to the enacted complex [26].

Tables 2. Kinetic parameters Ea*, ΔH*, ΔG* and ΔS* for carbon steel of pBut-g-PPD in 1N HCl at (10, 20 & 30 ppm).

Comp	conc	E_a	ΔH*	ΔS*	ΔG* (KJ.mol^{-1}.)		
		(KJ.mol^{-1})	(KJ.mol^{-1})	(J.k-1.mol^{-1})	298	308	323
Blank	36500	82.42	33.08	36.17	-10745.6	-11107.3	-11649.8
pBut -g- PPDA	10	91.4.92	44.24	27.23	-8070.3	-8342.6	-8751.05
	20	101.6	50.94	31.25	-9261.56	-9574.06	-10042.8
	30	102.2	64.33	33.63	-9957.41	-10293.7	-10798.2

4. *Study Thermal Analysis TGA for Inhibitor pBut-g-PPD*

Thermal gravimetric investigation (TGA) is one of the systems for thermal examination procedures used to contemplate the thermal stability of a wide assortment of materials. TGA measures the sum and step of progress in the mass of an example as a component of temperature or time a in an inert atmosphere [27, 28]. In the present investigation a large number of the of thermal stability capacities were determined from the got thermo grams as tangential decomposition temperature (starting disintegration temperature T_i), the level of deterioration temperature at half loss of the example weight (T_{50}), the temperature of last the decay (T_f), singe content toward

the finish of the decay procedure, the step of deterioration process and the enactment vitality for decay process which determined when the weight reduction proportions relying upon the Arrhenius equation [29]. The pBut -g-PPD Stabilization appeared 202 C °, and afterward it confirmed the investigation in three phases, the weight reduction in the primary stage 19% in second stage is 39% the debasement of polymer leaving the carbon buildup about 63%. Table 5 inhibitor polymer pBut-g-PPD findthat inhibitors polymer referenced stable thermally and up to a temperature (202˚C), and furthermore that we discover (T_{max}) (Temperature Decomposition) at (244˚C) which is a generally high level of heat, While the at (600˚C) where the compound leftover pace of up to 67%.

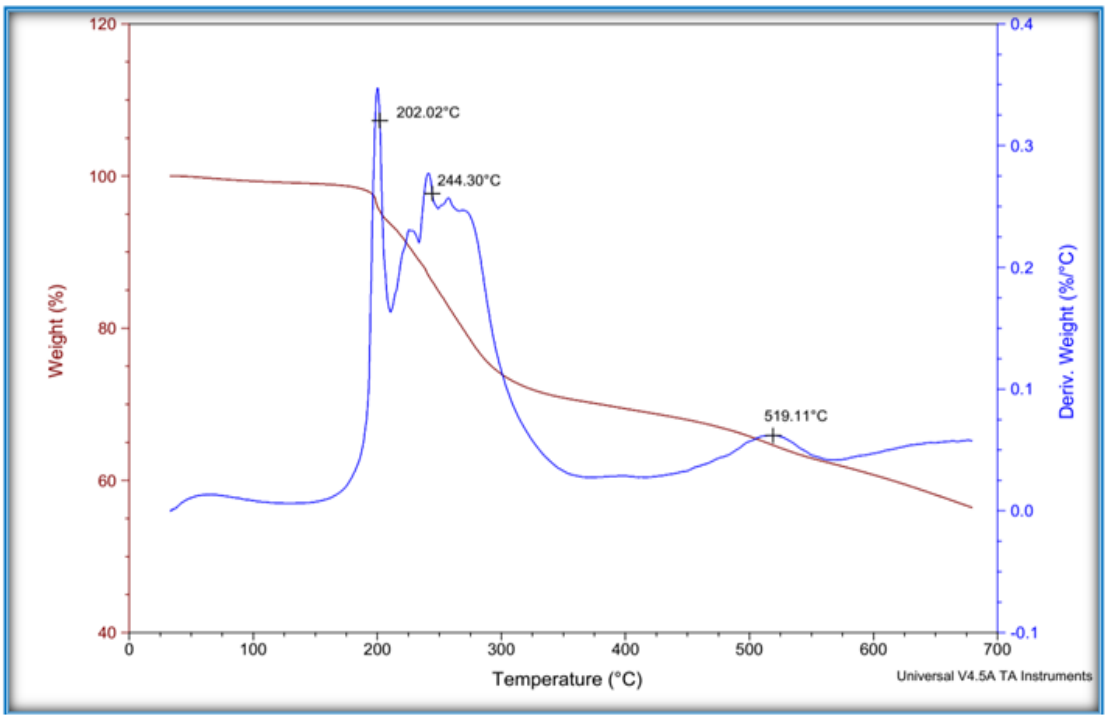

Fig. 17. The thermal analysis, TGA inhibitor the pBut-g-PPDA.

Table 3. The functions of thermal analysis TGA and DTA of pBut-g-PPDA.

polymer Code	Decomposition Stage	T_i C°	T_{op} C°	T_f C°	Rate of Decomp % w_t /min	Ruds. at 650 C°	T_{50} C°% Weight Loss
pBut-g- PPDA	First stage	160	202	225	0.292	700 >	67%
	Second stage	230	244	360	0.293		
	Third stage	480	519	550	0.557		

5. *Differential Scanning Calorimetry (DSC)*

Differential checking calorimetry can be utilized to quantify a number of trademark properties of an example. This system is applied generally for analyzing polymeric materials to decide their thermal transitions. The test experiences a physical change, for example, stage progress which is exothermic or endothermic relying upon the kind of sample [30]. Thermogram indicated an endothermic pinnacle 74 C° relating to the loss of alkali at around 213 C° the glass change temperature is showed up in a medium exothermic pack.

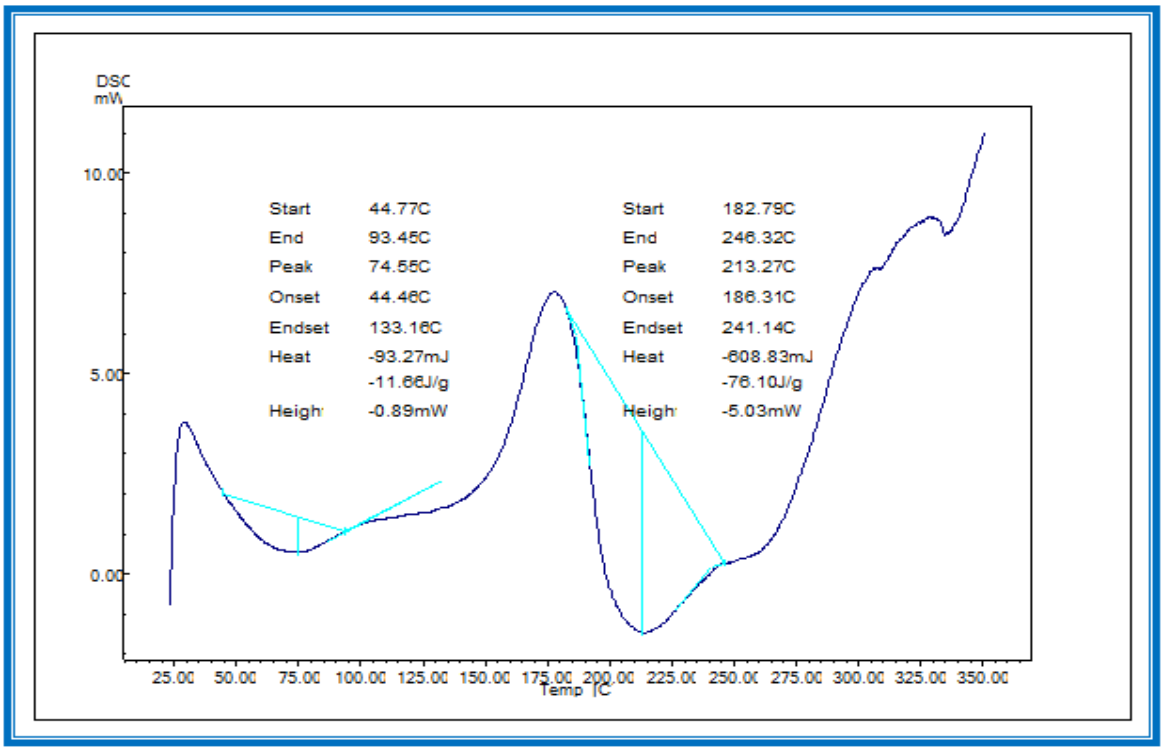

Fig. 18. DSC thermogram pBut-g-PPDA.

Table 4. The functions of thermal analysis TGA and DTA of pBut-g-PPDA.

Polymer	Phase Transition of decomposition Temperature							
	T_i	T_{op}	T_f	ΔH J/g	T_i	T_{op}	T_f	ΔH J/g
P3	44.7	74.5	93.4	-11.6	182	213	246	-76.1

IV. Conclusion

Polybutadiene-g-paraphynlene diamine new from ground tire rubbere go about as corrosion inhibitors of carbon steel in 1N HCl arrangements. The restraint productivity increments with increment in inhibitors concentrations and diminishes with raising temperature. The explored mixes were blended sort inhibitors. The adsorption of the examined compound on carbon steel surface in HCl arrangement. The negative estimations of ΔG promotions show the suddenness of the adsorption procedure. The parameter of adsorption free initiation vitality ΔG_0 promotions shows that the adsorption of inhibitor includes chemisorption.

References

[1] A.M. Al-Turkustani, S.T. Arab, A.A. Al-Reheli, Corrosion and corrosion inhibition of mild steel in H2SO4 solutions by zizyphus spina-christi as green inhibitor, International Journal of Chemistry, 2 (2010).
[2] B. Rani, B.B.J. Basu, Green inhibitors for corrosion protection of metals and alloys: an overview, International Journal of corrosion, 2012 (2012).
[3] Y. Song, J. Liu, H. Wang, H. Shu, Research Progress of Nitrite Corrosion Inhibitor in Concrete, International Journal of Corrosion, 2019 (2019).
[4] H. Ziari, H. Divandari, M. Hajiloo, A. Amini, Investigating the effect of amorphous carbon powder on the moisture sensitivity, fatigue performance and rutting resistance of rubberized asphalt concrete mixtures, Construction and Building Materials, 217 (2019) 62-72.
[5] Z. Enquan, W. Qiong, Experimental Investigation on Shear Strength and Liquefaction Potential of Rubber-Sand Mixtures, Advances in Civil Engineering, 2019 (2019).
[6] K. Formela, D. Wąsowicz, M. Formela, A. Hejna, J. Haponiuk, Curing characteristics, mechanical and thermal properties of reclaimed ground tire rubber cured with various vulcanizing systems, Iranian Polymer Journal, 24 (2015) 289-297.
[7] N. Amenaghawon, F. Aisien, O. Agho, Application of recycled rubber from scrap tyres in the adsorption of toluene from aqueous solution, Journal of Applied Sciences and Environmental Management, 17 (2013) 411-417.

[8] Ł. Piszczyk, A. Hejna, M. Danowska, M. Strankowski, K. Formela, Polyurethane/ground tire rubber composite foams based on polyglycerol: processing, mechanical and thermal properties, Journal of Reinforced Plastics and Composites, 34 (2015) 708-717.
[9] D. Quy Huong, T. Duong, P.C. Nam, Effect of the Structure and Temperature on Corrosion Inhibition of Thiourea Derivatives in 1.0 M HCl Solution, ACS omega, 4 (2019) 14478-14489.
[10] A. Ammar, M. Shahid, M. Ahmed, M. Khan, A. Khalid, Z. Khan, Electrochemical study of polymer and ceramic-based nanocomposite coatings for corrosion protection of cast iron pipeline, Materials, 11 (2018) 332.
[11] A. Fouda, A.H. El-Azaly, R. Awad, A. Ahmed, New benzonitrile azo dyes as corrosion inhibitors for carbon steel in hydrochloric acid solutions, Int. J. Electrochem. Sci, 9 (2014) 1117-1131.
[12] A. Kakaroglou, B. Nisol, T. Hauffman, I. De Graeve, F. Reniers, G. Van Assche, H. Terryn, Incorporation of corrosion inhibitor in plasma polymerized allyl methacrylate coatings and evaluation of its corrosion performance, Surface and Coatings Technology, 259 (2014) 714-724.
[13] Y. Abboud, A. Abourriche, T. Saffaj, M. Berrada, M. Charrouf, A. Bennamara, H. Hannache, A novel azo dye, 8-quinolinol-5-azoantipyrine as corrosion inhibitor for mild steel in acidic media, Desalination, 237 (2009) 175-189.
[14] T.W. Quadri, L.O. Olasunkanmi, O.E. Fayemi, M.M. Solomon, E.E. Ebenso, Zinc oxide nanocomposites of selected polymers: synthesis, characterization, and corrosion inhibition studies on mild steel in HCl solution, ACS Omega, 2 (2017) 8421-8437.
[15] P. Singh, M. Quraishi, S. Gupta, A. Dandia, Investigation of the corrosion inhibition effect of 3-methyl-6-oxo-4-(thiophen-2-yl)-4, 5, 6, 7-tetrahydro-2H-pyrazolo [3, 4-b] pyridine-5-carbonitrile (TPP) on mild steel in hydrochloric acid, Journal of Taibah University for Science, 10 (2016) 139-147.
[16] S.R. Scagliusi, E.C. Cardoso, C.A. Pozenato, A.B. Lugão, Degrading radiation effects on properties of bromobutyl rubber compounds.
[17] D.C. Greminger, R.B. Leng, W.G. Stobby, S.I. Kram, Process for brominating butadiene/vinyl aromatic copolymers, Google Patents, 2012.
[18] H. Kawaguchi, P. Loeffler, O. Vogl, Head-to-head polymers: 33. Bromination of cis-1, 4-polybutadiene to head-to-head poly (vinyl bromide), Polymer, 26 (1985) 1257-1264.
[19] M.R. Ibrahim, H.Y. Katman, M.R. Karim, S. Koting, N.S. Mashaan, a review on the effect of crumb rubber addition to the rheology of crumb rubber modified bitumen, Advances in Materials Science and Engineering, 2013 (2013).
[20] J. Elena, M.D. Lucia, Application of X-ray diffraction (XRD) and scanning electron microscopy (SEM) methods to the portland cement hydration processes, Journal of Applied Engineering Sciences, 2 (2012) 35-42.
[21] L.-C. Jia, Y.-K. Li, D.-X. Yan, Flexible and efficient electromagnetic interference shielding materials from ground tire rubber, Carbon, 121 (2017) 267-273.
[22] K. Raviprabha, R.S. Bhat, Inhibition Effects of Ethyl-2-Amino-4-Methyl-1, 3-Thiazole-5-Carboxylate on the Corrosion of AA6061 Alloy in Hydrochloric Acid Media, Journal of Failure Analysis and Prevention, 19 (2019) 1464-1474.
[23] P. Kumari, P. Shetty, S.A. Rao, Corrosion protection properties of 4-hydroxy-N'-[(1E, 2E)-3-phenylprop-2-en-1-ylidene] benzohydrazide on mild steel in hydrochloric acid medium, Protection of Metals and Physical Chemistry of Surfaces, 51 (2015) 1034-1042.
[24] R.S. Oguike, Corrosion studies on stainless steel (FE6956) in hydrochloric acid solution, Advances in Materials Physics and Chemistry, 4 (2014) 153.
[25] H. Zarrok, A. Zarrouk, R. Salghi, M.E. Touhami, H. Oudda, B. Hammouti, R. Touir, F. Bentiss, S. Al-Deyab, Corrosion inhibition of C38 steel in acidic medium using N-1 naphthylethylenediamine dihydrochloride monomethanolate, Int. J. Electrochem. Sci., 8 (2013) 6014-6032.
[26] A. Kadhum, A. Mohamad, L. Hammed, A. Al-Amiery, N. San, A. Musa, Inhibition of mild steel corrosion in hydrochloric acid solution by new coumarin, Materials, 7 (2014) 4335-4348.
[27] P. Poddar, M.S. Islam, S. Sultana, H. Nur, A. Chowdhury, Mechanical and thermal properties of short arecanut leaf sheath fiber reinforced polypropyline composites: TGA, DSC and SEM analysis, Journal of Material Science and Engineering, 5 (2016) 270.
[28] C. De Blasio, Thermogravimetric Analysis (TGA), Fundamentals of Biofuels Engineering and Technology, Springer2019, pp. 91-102.
[29] J. Cai, D. Xu, Z. Dong, X. Yu, Y. Yang, S.W. Banks, A.V. Bridgwater, Processing thermogravimetric analysis data for isoconversional kinetic analysis of lignocellulosic biomass pyrolysis: Case study of corn stalk, Renewable and Sustainable Energy Reviews, 82 (2018) 2705-2715.
[30] T.C. Chiang, S. Hamdan, M.S. Osman, Urea formaldehyde composites reinforced with Sago fibres analysis by FTIR, TGA, and DSC, Advances in Materials Science and Engineering, 2016 (2016).

AUTHOR'S PROFILE

First Author
Khawlah S. Burghal, Chemistry Department, Science College, Basrah University, Basrah, Iraq.

Second Author
Hassan T. Abdulsahib, Chemistry Department, Science College, Basrah University, Basrah, Iraq.

Third Author
Sameerah A. Zearah, Chemistry Department, Science College, Basrah University, Basrah, Iraq.